

In-Orbit SAR Performance of TerraSAR-X and TanDEM-X Satellites

Thomas Kraus⁽¹⁾, Dirk Schrank⁽¹⁾, Paola Rizzoli⁽¹⁾, Benjamin Bräutigam⁽¹⁾

⁽¹⁾ Microwaves and Radar Institute, German Aerospace Center (DLR), Münchner Straße 20, 82234 Oberpfaffenhofen, Germany, T.Kraus@dlr.de

Abstract

TerraSAR-X was successfully launched and commissioned in 2007. Since that time it is acquiring highly accurate and reliable SAR products for scientific and commercial applications. The performance of these SAR images is monitored regularly and in detail. These data provided an outstanding basis for the commissioning phase activities of calibration and performance evaluation of TanDEM-X in 2010. This paper focuses on monostatic performance parameters evaluated for TanDEM-X with TerraSAR-X as a reference.

1. Introduction

The TanDEM-X satellite (TDX) is a rebuild of the TerraSAR-X satellite (TSX) [1] with some special equipment and options to support the close formation flight necessary to form a free flying space interferometer [2]. It is designed to achieve comparable performance measures for TDX as they are obtained by TSX since its launch in 2007. From missions point of view this is important for two reasons. First the monostatic TerraSAR-X mission has to be continued with constant quality on both satellites [3]. Secondly a good performance of both instruments is important for the simultaneous operation in the bistatic TanDEM-X mission in order to generate high quality interferograms and digital elevation models (DEMs) [4, 5].

After TDX had been launched on June 21st, 2010, its commissioning phase has been partitioned into three main phases [6]. The first one included the launch and the drift of TDX towards TSX in order to obtain the formation for the pursuit monostatic commissioning phase. This constellation was characterized by a 20 km along track separation of both satellites. Hereby TDX followed TSX on an orbit which allowed acquiring SAR images of the same ground tracks as TSX with an almost identical geometry but a time lag of approximately three seconds. Most of the data presented in the following sections were acquired during this phase which lasted about ten weeks. After its successful monostatic commissioning, TDX further drifted towards TSX until both satellites were in close formation. So the bistatic commissioning and finally the operational TanDEM-X phase could start. From the point both satellites reached close formation, TDX started to support the monostatic TerraSAR-X mission operationally.

In this paper some key SAR performance parameters from [7] for both radar instruments of the satellites TSX and TDX will be discussed. In particular a comparison of the point target analysis between both sensors will be shown in section 2, followed by a treatment of the noise equivalent sigma zero (NESZ) characteristics in section 3. The accuracy of repeat pass acquisitions with respect to their orbital position will be discussed because of its importance especially for repeat pass interferometry (section 4). The subsequent section is on the attitude steering accuracy influencing the total zero Doppler steering [8] and so the Doppler centroid. The paper is closed with an example of inter-satellite interference between both satellites which occurred during the monostatic commissioning phase.

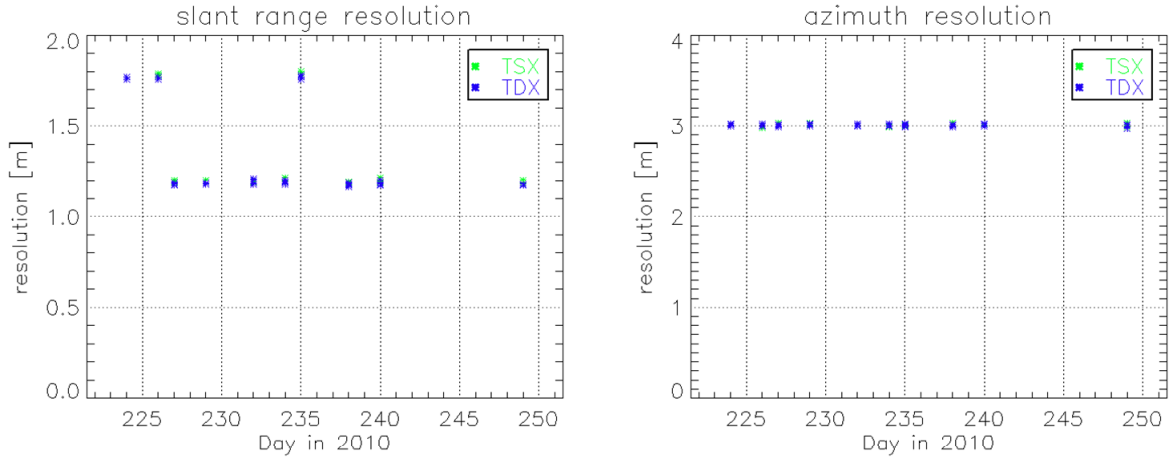


Figure 1: Slant range (left Fig.) and azimuth resolution (right Fig.) of SSC images for both satellites. There are 122 measurements derived from 19 SSC images acquired on ten days in 2010.

2. Point Target Analysis

During the pursuit monostatic commissioning phase of TDX an extensive calibration campaign for the SAR instrument was carried out, including acquisitions over point targets with different antenna beams [9, 10]. For comparative reasons each acquisition was performed by TSX in the same pass, too. From these measurements the resolution and the side lobe ratios can be determined. In total 122 point targets were analyzed, 64 for TDX and 58 for TSX.

Figure 1 shows the resolutions in slant range and azimuth direction for both satellites. Both SAR systems achieve an almost identical slant range resolution of 1.2 m at a bandwidth of 150 MHz and 1.8 m range resolution with 100 MHz bandwidth. The azimuth resolution is range independent and identical for both systems.

The resolution is defined by image processing with a Hamming weighting (α coefficient 0.6) in order to reduce the peak-to-side lobe ratio (PSLR) to under -25 dB (peak). As can be seen in Fig. 2 this limit is almost always met. The few outliers in the PSLR can be explained by strong natural scatterers in the vicinity of the target since they occur for TSX and TDX simultaneously. The integrated side lobe ratio (ISLR) has been verified with the same point targets. This parameter also meets its goal of -18 dB with measured values around -19.6 dB (mean) and a standard deviation of less than 0.6 dB.

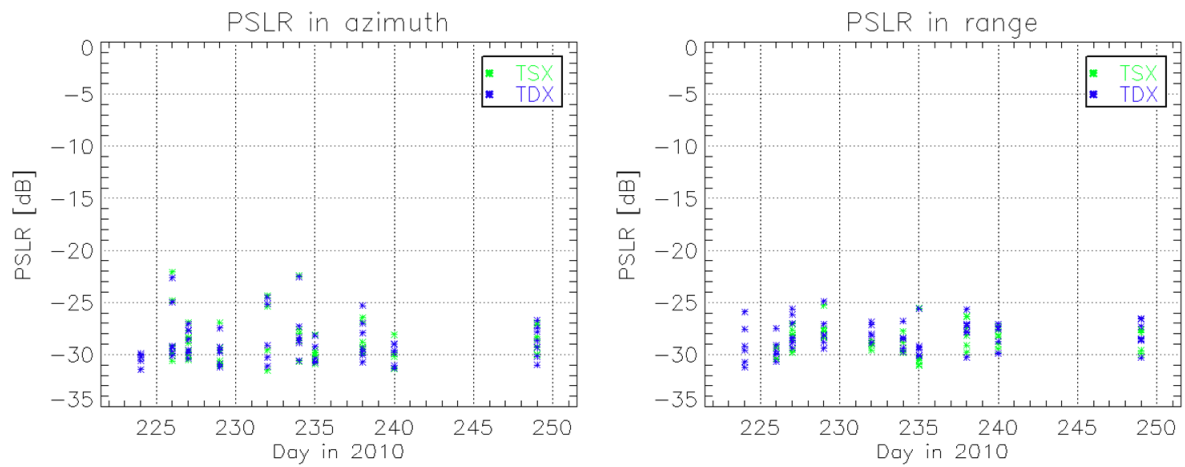


Figure 2: Peak-to-side lobe ratio in range (left fig.) and azimuth (right fig.) of SSC images for both satellites.

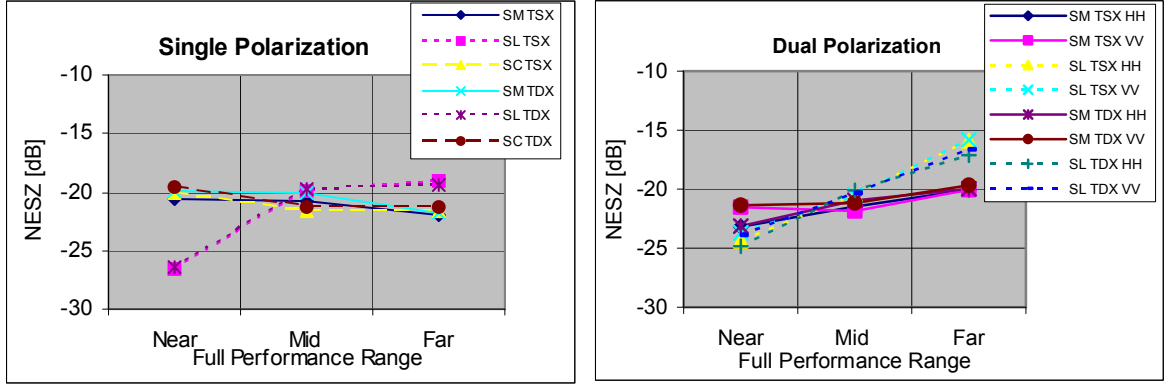


Figure 3: NESZ characteristics for TSX and TDX for single and dual polarization acquisitions derived from distributed targets. Near, mid and far range is referred to the TerraSAR-X full performance range [7], corresponding to an incidence angle range of 19.7 to 45.5 degree in Stripmap (SM) and ScanSAR (SC) and up to 55.2 degree in Spotlight (SL) mode.

3. NESZ Characteristics

The noise equivalent sigma zero (NESZ) level of a SAR system is a key driver for its signal-to-noise ratio characteristics. There are two different approaches to derive the NESZ from TerraSAR-X level 1b products. The first is to take the annotated noise profiles directly from the annotation files. These profiles are based on noise-only measurements [11] before and after image acquisition. The second way is to analyze distributed targets on areas having low backscatter like rivers and lakes where the received signal is assumed to be dominated by instrument noise.

For the results presented in this paper the second method was used. Fig. 3 shows the NESZ to be well below its specified value of -19 dB [7] for single polarization and for most cases of dual polarization. The outliers are measurements in Spotlight mode with dual polarization and a large incidence angle. These measurements are very likely to be affected by range ambiguities. Nevertheless also the NESZ behaviour is very similar for TSX and TDX.

4. Repeat-Pass Accuracy

For repeat-pass interferometry, especially in ScanSAR mode, it is extremely important to start each acquisition exactly at the same orbital (along-track) position. An onboard start time correction mechanism triggers the start of each data take based on in-orbit GPS measurements. The along-track separation in meters of the start position of several hundred repeat-pass acquisition pairs is depicted in Fig. 4. The results show TSX and TDX to have comparable repeatability capabilities for consecutive pairs of data takes. The difference is below 50 m for all pairs, ensuring more than 90% of ScanSAR burst overlap [7].

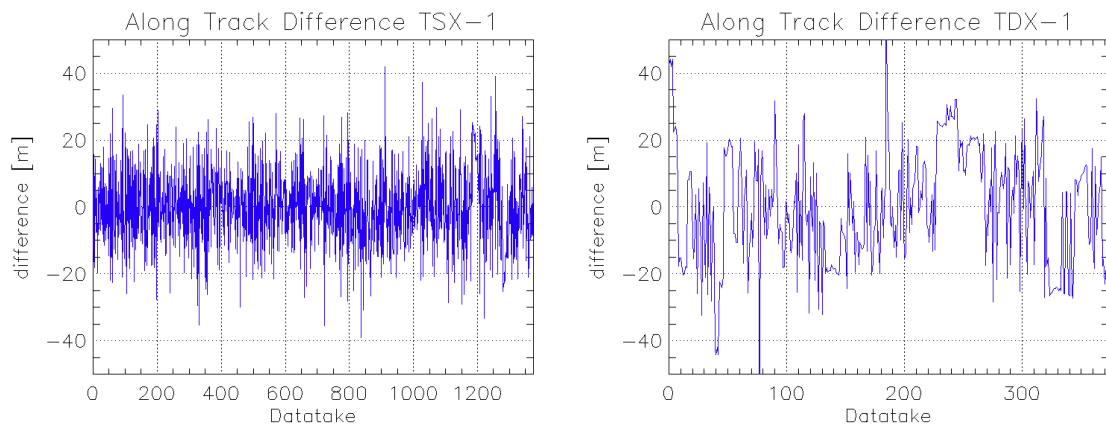


Figure 4: Along tack separation between the start positions of repeat-pass pairs of data takes.

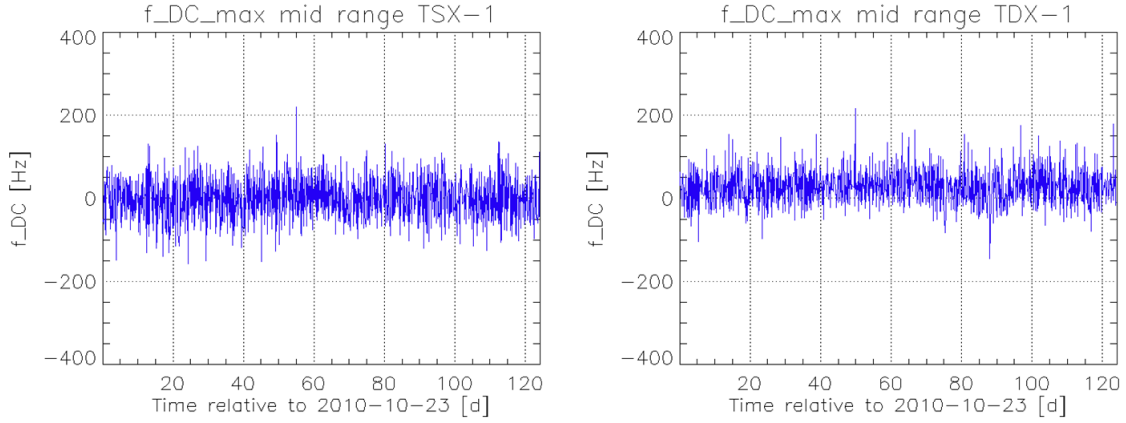


Figure 5: Maximum Doppler centroid for the mid range of each swath of a data take; left TSX, right TDX.

It has to be mentioned that TSX follows its fixed reference orbit within the orbit tube since its launch. For TDX this is not true. The TDX reference orbit is not constant but changing over time since for the generation of the global DEM several acquisitions with different baselines are intended. However, for the pursuit monostatic phase – and so the analysis presented here – the TDX orbits were the same for every eleven day repeat cycle.

5. Attitude Steering Performance

TSX and TDX perform total zero Doppler steering [8] in order to minimize the Doppler centroid. This is mainly a steering in yaw but also in pitch direction. Analysis of the measured attitude data (star trackers) shows the error between commanded and real attitude to be well below the requirement of 60 arc seconds for all three axes. This accuracy enables a very small and stable Doppler centroid. In Fig. 5 the maximum measured Doppler centroid for the mid range of the swath of an acquisition is depicted. The left figure contains 2210 measurements corresponding to the same number of acquisitions of TSX for the time period from the end of October 2010 till the end of February 2011. For TDX 1760 measurements are depicted on the right respectively. The root mean square (RMS) measures are 43.2 Hz for TSX and 45.6 Hz for TDX. These results are in accordance to the limit of 120 Hz [7] and highly appreciated for Spotlight imaging and interferometry [12].

6. Inter Satellite Interference

During the pursuit monostatic phase TDX was following TSX with an along track separation of 20 km which corresponds to about three seconds. In order to acquire an interferometric pair of images both satellites were commanded identically which means with the same timing. However the start of each monostatic acquisition was triggered by the position derived from onboard GPS measurements (cf. chap. 4) and therefore the timing was not synchronous. This asynchronous operation led to interference by radar pulses radiated from the other satellite. One example is depicted in Fig. 6 on the left where the bright line in the middle of the swath is clearly visible. It ends 20 km before the end of the image since TSX started – and so finishes – its acquisition three seconds earlier.

As a consequence, after the effect was recognized the transmit pulse chirp slope of TDX was set to up-chirp while TSX stayed on down-chirp. This measure does not prevent the interference. The signal energy is still received (right part of Fig. 6), but the interference does no longer focus in the image.

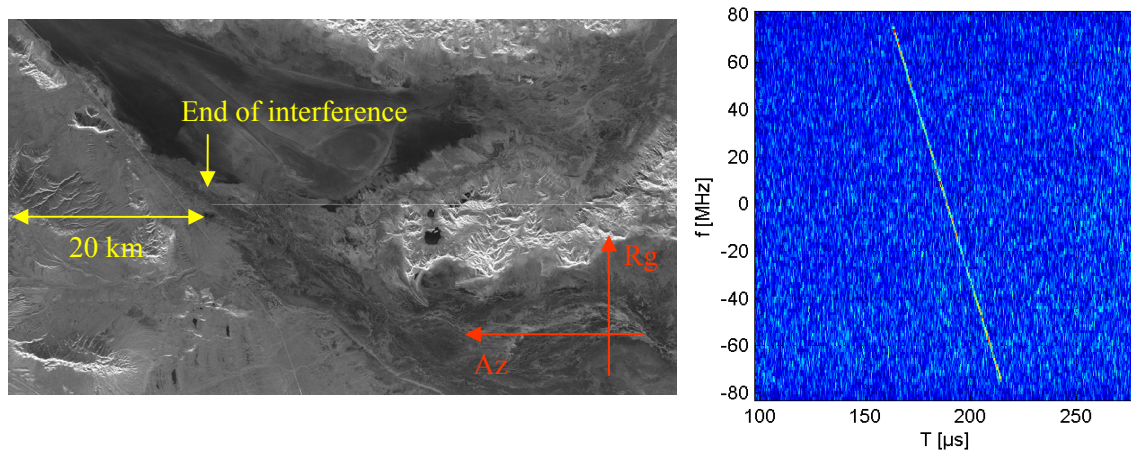


Figure 6: TDX monostatic Stripmap image of Black Rock desert, NV with interference from TSX; spectrogram of a receive-only (noise) measurement by TDX containing a 150 MHz down-chirp of 50 μ s duration transmitted by TSX.

After transition to the close formation [6] there are two configurations the instruments can operate in. Either in monostatic mode which means only one instrument is operating, the other one is inactive. The other mode – the bistatic one – relies on a synchronous operation of both radars. So an asynchronous, simultaneous operation like in the pursuit monostatic commissioning phase is not foreseen during nominal monostatic or bistatic operation. Therefore the antipodal chirp solution was considered adequate for the short pursuit monostatic commissioning phase. This solution maintained the ability to trigger the acquisitions by the GPS based onboard mechanism which ensures the best possible overlap of both independent acquisitions.

7. Conclusion

The TanDEM-X satellite was launched in June 2010 and underwent an extensive commissioning and calibration campaign. As TDX is almost an identical rebuilt of TSX it was expected to achieve SAR products with similar quality. A detailed analysis of the performance parameters for TDX was carried out with TSX as a very accurate and stable reference. In this paper the results for some key performance measures were presented:

- point target analysis
- NESZ characteristics
- repeat-pass accuracy
- attitude steering performance

Additionally the effect of interference – which occurred only for the pursuit monostatic constellation – was depicted and an adequate method for its mitigation presented.

From these analyses it can be concluded that the performance parameters of TDX are within the performance specification of the TerraSAR-X mission and further more the satellite is fully capable to act as part of the TanDEM-X interferometer.

Acknowledgments

The TanDEM-X project is partly funded by the German Federal Ministry for Economics and Technology (Förderkennzeichen 50 EE 1035).

References

- [1] R. Werninghaus, S. Buckreuss, „The TerraSAR-X mission and system design“, *IEEE Trans. Geosci. Remote Sens.*, vol. 48, No. 2, pp. 606-614, 2010

- [2] A. Moreira, G. Krieger, I. Hajnsek, D. Hounam, M. Werner, S. Riegger, E. Settelmeier, "TanDEM-X: A TerraSAR-X add-on satellite for single-pass SAR interferometry", in *Proc. IGARSS*, Anchorage, AK, Vol. 2, pp. 1000-1003, 2004
- [3] B. Bräutigam, P. Rizzoli, C. Gonzalez, M. Weigt, D. Schrank, D. Schulze, M. Schwerdt, "SAR performance monitoring for TerraSAR-X mission", in *Proc. IGARSS*, Honolulu, Hawaii, Vol. 30, pp. 3454-3457, 2010
- [4] M. Martone, P. Rizzoli, B. Bräutigam, G. Krieger, „First interferometric performance results of TanDEM-X commissioning phase“, *URSI-F-Triennial Symposium*, Garmisch-Partenkirchen, Germany, 2011.
- [5] G. Krieger, A. Moreira, H. Fiedler, I. Hajnsek, M. Werner, M. Younis, M. Zink, „TanDEM-X: A satellite formation for high-resolution SAR interferometry“, *IEEE Trans. Geosci. Remote Sens.*, vol. 45, No. 11, pp. 3317-3341, 2007
- [6] J. Hueso Gonzalez, M. Bachmann, H. Hofmann, "TanDEM-X commissioning phase status", in *Proc. IGARSS*, Honolulu, Hawaii, Vol. 30, pp. 2633-2635, 2010
- [7] T. Fritz, M. Eineder, "TerraSAR-X basic product specification document", 2010
- [8] H. Fiedler, E. Boerner, J. Mittermayer, G. Krieger, „Total zero Doppler steering – a new method for minimizing the Doppler centroid“, *IEEE Geosci. Remote Sens. Lett.*, vol. 2, No. 2, pp. 141-145, 2005
- [9] M. Schwerdt, J. Hueso Gonzalez, M. Bachmann, D. Schrank, C. Schulz, B. Döring, "Monostatic calibration of both TanDEM-X satellites", in *Proc. IGARSS*, Honolulu, Hawaii, Vol. 30, pp. 2636-2639, 2010
- [10] M. Schwerdt, B. Bräutigam, M. Bachmann, B. Döring, D. Schrank, J. Hueso Gonzalez, „Final TerraSAR-X calibration results based on novel efficient methods“, *IEEE Trans. Geosci. Remote Sens.*, vol. 48, No. 2, pp. 677-689, 2010
- [11] B. Bräutigam, J. Hueso Gonzalez, M. Schwerdt, M. Bachmann, "TerraSAR-X instrument calibration results and extension for TanDEM-X", *IEEE Trans. Geosci. Remote Sens.*, vol. 48, No. 2, pp. 702-715, 2010
- [12] M. Eineder, N. Adam, R. Bamler, N. Yague-Martinez, H. Breit, "Spaceborne Spotlight SAR interferometry with TerraSAR-X", *IEEE Trans. Geosci. Remote Sens.*, vol. 47, No. 5, pp. 1524-1535, 2009